Hindawi Publishing Corporation
Science and Technology of Nuclear Installations
Volume 2013, Article ID 402570, 10 pages
http://dx.doi.org/10.1155/2013/402570

Research Article

A Solution-Based Approach for Mo-99 Production: Considerations for Nitrate versus Sulfate Media

Amanda J. Youker, Sergey D. Chemerisov, Michael Kalensky, Peter Tkac, Delbert L. Bowers, and George F. Vandegrift

Chemical Sciences and Engineering Division, Argonne National Laboratory, 9700 S. Cass Avenue, Argonne, IL 60439, USA

Correspondence should be addressed to Amanda J. Youker; youker@anl.gov

Received 17 June 2013; Accepted 7 August 2013

Academic Editor: Mushtaq Ahmad

Molybdenum-99 is the parent of Technetium-99m, which is used in nearly 80% of all nuclear medicine procedures. The medical community has been plagued by Mo-99 shortages due to aging reactors, such as the NRU (National Research Universal) reactor in Canada. There are currently no US producers of Mo-99, and NRU is scheduled for shutdown in 2016, which means that another Mo-99 shortage is imminent unless a potential domestic Mo-99 producer fills the void. Argonne National Laboratory is assisting two potential domestic suppliers of Mo-99 by examining the effects of a uranyl nitrate versus a uranyl sulfate target solution configuration on Mo-99 production. Uranyl nitrate solutions are easier to prepare and do not generate detectable amounts of peroxide upon irradiation, but a high radiation field can lead to a large increase in pH, which can lead to the precipitation of fission products and uranyl hydroxides. Uranyl sulfate solutions are more difficult to prepare, and enough peroxide is generated during irradiation to cause precipitation of uranyl peroxide, but this can be prevented by adding a catalyst to the solution. A titania sorbent can be used to recover Mo-99 from a highly concentrated uranyl nitrate or uranyl sulfate solution; however, different approaches must be taken to prevent precipitation during Mo-99 production.

1. Introduction

Argonne is assisting two potential domestic suppliers of Molybdenum-99, and both plan to use a fissioning LEU solution as either uranyl nitrate or uranyl sulfate to produce Mo-99. Babcock and Wilcox Technical Services Group (BWTSG) is developing an aqueous homogeneous reactor (AHR) for Mo-99 production, which will utilize an LEU fuel (19.75% U-235) as uranyl nitrate. Their system is referred to as MIPS (Medical Isotope Production System) [1]. SHINE Medical Technologies is developing Subcritical Hybrid Intense Neutron Emitter (SHINE), which is an accelerator-driven process that will use an LEU uranyl sulfate target solution for Mo-99 production [2, 3]. For these systems, Argonne has developed a Mo-recovery process for either the irradiated uranyl sulfate or uranyl nitrate solution using a titania sorbent [4–16].

Solution preparation is much easier for MIPS compared to SHINE [13, 15]. The differences in procedures will be discussed in more detail below.

Uranyl nitrate and uranyl sulfate solutions have been irradiated at the Argonne 3 MeV Van de Graaff accelerator to study the effects of a high radiation field on solution chemistry, specifically related to pH changes, peroxide formation, and molybdenum and iodine redox chemistry. The effect of a high radiation field caused significant pH changes in a uranyl nitrate solution, which resulted from the radiolysis of nitrate to form a variety of reduced nitrogen species from nitrite to NO_x gases and to ammonia [17]. Uranium and fission product precipitation becomes a concern when the pH rises above 3 [1]. As a result, nitric acid will need to be added periodically to the uranyl nitrate MIPS fuel solution during operation to prevent large pH increases that may lead to the precipitation of some fission products and eventually uranium. The pH of a uranyl sulfate solution decreased postirradiation due to water loss from radiolysis [18]. Uranyl peroxide precipitated during irradiation of uranyl sulfate solutions that did not contain catalysts. Ferrous and ferric sulfate, cupric sulfate, potassium iodide, 304 stainless steel turnings, and Zr metal have been

tested as potential catalysts for peroxide destruction during irradiation of uranyl sulfate solutions [19].

Although molybdenum can be recovered from both uranyl nitrate and uranyl sulfate solutions, the task is easier from nitrate media. This is most easily seen by comparing Mo(VI) partitioning between the solutions and the titania sorbent [4, 8, 13–15, 20]. However, plant-scale separation columns have been designed for both MIPS and SHINE systems [8, 9, 12–15]. A general comparison of the two recovery operations will be discussed below. New data to be discussed in this paper are column experiments performed using uranyl sulfate solutions spiked with tracer Mo-99 and stable Mo added as sodium molybdate under a constant radiation dose at the Van de Graaff [21]. Additionally, results from Van de Graaff iodine speciation experiments in nitrate and sulfate media will also be presented [21]. However, the Van de Graaff iodine results do not agree with iodine results obtained using dissolved, irradiated foils added as a spike to a uranyl sulfate solution.

2. Materials and Methods

2.1. Materials. Depleted-uranium metal plates were used to prepare uranyl nitrate and uranyl sulfate solutions. The plates were approximately $2'' \times 2''$ with a width of $1/8''$ and a mass of ~150 g. Concentrated nitric acid and sulfuric acid were obtained from Sigma-Aldrich, and dilutions were made to prepare solutions with different acid concentrations required for the various steps in the uranyl-salt solution-preparation processes. Pure titania sorbents (Sachtopore Normal Phase—110 and 40 micron particle size) were obtained from Zirchrom Separations, Inc. Sodium molybdate was obtained from Sigma-Aldrich, and Mo-99 was milked from a Lantheus spent Tc-99m generator. 30% hydrogen peroxide was used as received from Sigma-Aldrich. A 3 MeV Van de Graaff (VDG) accelerator was used to generate a radiation field.

2.2. Methods. Uranyl nitrate solutions were prepared by dissolving uranium-metal plates in 8 M nitric acid using a reaction kettle, equipped with a heating mantle, kettle cover, and reflux condenser. The uranyl nitrate solution was brought to dryness several times to drive off excess nitric acid and redissolved in a mixture of nitric acid and water until a final pH of 1.0 was reached at the desired uranium concentration.

Two different avenues have been investigated for the preparation of uranyl sulfate. In the first method of preparation, uranium metal is converted to uranyl nitrate, and heat and sulfuric acid are added to drive off nitrate and form uranyl sulfate. Sulfuric acid (1–18 M) is added directly to the uranyl nitrate solid to prepare uranyl sulfate. A rotary evaporator with a water-cooled condenser kept under constant vacuum is used to facilitate conversion from nitrate to sulfate. An oil bath is used to heat the solution to drive off nitric acid and thus to convert the salt to uranyl sulfate. The second method of preparation involves oxidizing U metal to U_3O_8, forming uranyl peroxide, and redissolving it in dilute sulfuric acid. Uranium metal is oxidized in a furnace at a temperature near 720°C for full conversion and usually takes about 24 h for a single metal plate (~150 g). Approximately 5 mL of 30% H_2O_2 per gram of U_3O_8 and a stoichiometric amount of H_2SO_4 are added to the U_3O_8 with heat. Complete conversion to uranyl peroxide occurs in about 40 minutes for a 50 g-U batch, and the solid product is redissolved in dilute sulfuric acid with heat. Complete dissolution of a 50 g-U batch takes about 1 hour.

Uranium solutions and titania columns were irradiated for 1 hour using the Van de Graaff as a radiation source. Each uranium solution was passed through a titania column over a period of 2 hours, while under a constant radiation dose, uranium solution and titania column were both in the radiation field. Column sizes and experimental parameters are direct downscale designs of the plant-scale designs generated by Versatile Reaction Separation (VERSE) for the SHINE process. The purpose of these experiments was to determine whether a radiation dose of approximately 70 kRad/h caused a change in Mo redox chemistry. After the target solution was loaded onto the column, it was washed with acid and water, and Mo-99 was recovered using 0.1 M NaOH heated to 70°C. Column wash and strip steps were not performed in a radiation field.

Column experiments were performed under a constant radiation dose using a Fluid Metering Inc. (FMI) pump and a stainless steel column at the Van de Graaff. Subsequent wash and Mo elution steps were carried out using an ÄKTA liquid chromatography system. Column and solution temperatures were kept at 80°C except for the Mo strip solution, which was kept at 70°C. Feed solution was loaded in the upflow direction to concentrate Mo at the base of the column and in the case of irradiated solutions, to prevent entrapment of fission gases that may potentially generate channels in the column. The column was washed with acid (0.1–1 M) and then water. Mo was eluted using 0.1 M NaOH heated to 70°C, and a final water wash was performed.

The experimental setup for measuring radiolytic-gas generation and peroxide formation with/without the presence of catalysts was designed with two interconnected systems—the process loop and the sampling manifold. The process loop is a closed loop of stainless steel tubing that consists of a quartz target vessel for the sample, the electron beam, and a peristaltic pump. The target sample is inserted into a holder directly in the accelerator electron-beam path. The holder is attached to a recirculating pump and water bath to provide continuous cooling of the sample. The electron beam impinges on the cooling water and quartz tube in the setup. The 3.0 MeV Van de Graaff accelerator electron beam emits electrons and some X-rays, which interact with the sample. The sample tube has an inlet and outlet valve to recirculate headspace gases throughout the process loop. The sampling manifold is connected to the process loop by a bellows valve. The sampling manifold consists of a capacitance monometer, vacuum pump, and two analytical instruments connected by stainless steel tubing and a series of valves used to either evacuate, measure pressure, or analyze the gaseous constituents in the manifold. The gases are analyzed using a SRI-8610C gas chromatograph with a Thermal Conductivity Detector (TCD) and a Helium Ionization Detector (HID).

Separation is achieved with a 13X molecular sieve column and a Haysep-d column.

A 2 mL test solution is placed in a quartz sample tube. The sample tube is connected to the process loop in the beam path. The system is then evacuated and purged with helium several times to remove atmospheric gases. The process loop is pressurized to 800 torr with Ultra High Purity (UHP) helium.

The 3.0 MeV electron beam is set to 20 μA, and the sample is irradiated for approximately five hours. At 30-minute intervals, a sample of the headspace gas is withdrawn into the evacuated "Sampling Manifold" for analysis. The gas removed is replaced with helium to keep a constant pressure in the system. Prior to these experiments, oxalic-acid dosimetry was performed to determine the approximate dose deposited into the sample [22].

Uranyl sulfate and uranyl nitrate solutions were tested at various concentrations. The pH of the solutions was measured at the end of irradiation. Several known catalysts for the autodestruction of hydrogen peroxide were also tested to determine if each one was a suitable option for peroxide destruction in sulfate solutions.

3. Results and Discussion

3.1. Solution Preparation. Preparation of uranyl nitrate is straightforward because uranium metal can be dissolved directly in nitric acid. Adjustment of pH is relatively easy to do for a uranyl nitrate solution because excess nitrate can be removed by evaporation of nitric acid or by calcining uranyl nitrate to produce oxide. On the other hand, uranium metal cannot be dissolved directly in sulfuric acid without the addition of an oxidizing agent [13, 15, 16, 23, 24]. As a result, additional steps are required for the preparation of uranyl sulfate. Two methods are currently being examined for the preparation of uranyl sulfate: (1) calcine U metal to UO_3/U_3O_8 and dissolve it in a mixture of H_2O_2 and H_2SO_4 with heat, (2) dissolve U metal in HNO_3, use a calcination process to convert uranyl nitrate to UO_3, and dissolve UO_3 in H_2SO_4 [13, 23–27]. Uranyl nitrate is more attractive than uranyl sulfate in terms of solution preparation; however, uranyl sulfate is the better choice in terms of neutron economy and pH stability [1–3, 28–31]. Changes in pH observed upon irradiation at the Van de Graaff for uranyl sulfate, and uranyl nitrate solutions are discussed in more detail in the gas analysis results section.

Because conversion of a uranyl nitrate solution to a uranyl sulfate solution using a rotary evaporator showed that approximately 1–5% nitrate remains in the final uranyl sulfate solution, we recommend thermal oxidation of uranium metal followed by dissolution directly of the uranium oxide in a mixture of hydrogen peroxide and sulfuric acid with heat.

3.2. Mo Recovery: Nitrate versus Sulfate Media. Batch-study results show that Mo adsorbs better on a titania sorbent in a nitrate media than in sulfate media [13, 20]. Sulfate competes more strongly with molybdenum for adsorption sites than nitrate. For example, batch studies were performed in sodium nitrate and sulfate solutions, with anion concentrations representing what would be present in a 150 g-U/L solution of each one. With Mo concentrations in the range expected for MIPS and SHINE (10^{-5}–10^{-6} M), the K_d, which is defined as the ratio of Mo adsorbed on the sorbent (mol/g) to the concentration of Mo in solution (mol/L), values for Mo in the presence of sodium nitrate are 1.7–2.2 times larger than in the presence of sodium sulfate (Table 1). Similar batch studies were performed in the presence of 150 g-U/L uranyl nitrate and uranyl sulfate solutions. Figure 1 shows a direct comparison between the amount of Mo adsorbed per gram of sorbent versus the amount in solution in the presence of uranyl nitrate and uranyl sulfate solutions, and results indicate that more Mo is adsorbed in the presence of a uranyl nitrate solution, especially as the Mo concentration increases.

Table 1: Distribution ratios for Mo in the presence of sodium sulfate and sodium nitrate solutions.

Initial Mo (M)	K_d, Mo (mL/g) 0.63 M Na_2SO_4	K_d, Mo (mL/g) 1.26 M $NaNO_3$
$1E-06$	4900	11000
$1E-05$	3400	7600
$5E-05$	3100	5200

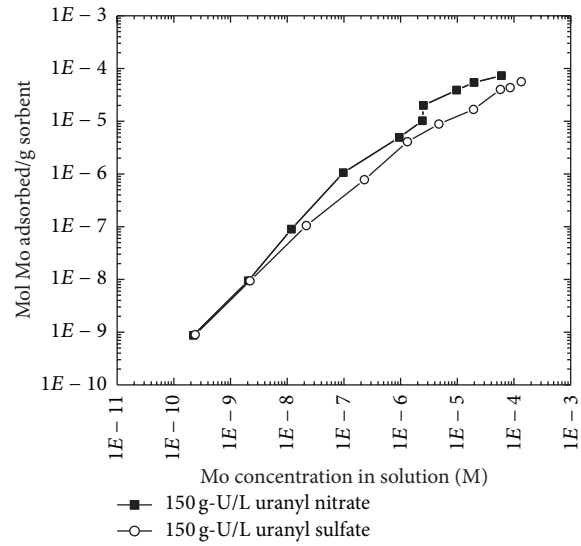

Figure 1: Amount of Mo adsorbed per gram of sorbent versus the amount in solution in the presence of solutions containing 150 g-U/L uranyl nitrate and 150 g-U/L uranyl sulfate.

3.3. Plant-Scale Column Designs. Batch data and small-scale column data for Mo adsorption in the presence of uranyl sulfate and uranyl nitrate solutions using a pure titania sorbent have been collected at Argonne and input into the VERSE simulator, which was developed by Dr. Wang at Purdue University [32]. VERSE takes data obtained in a batch mode and small-scale column setting to design a column for a large-scale separation process. Plant-scale columns have been designed for the MIPS (uranyl nitrate) and SHINE (uranyl sulfate) systems. Based on the batch data shown above, the Mo-recovery column is going to be larger for the SHINE system due to competition from sulfate. Table 2 shows

Table 2: Plant-scale column designs for MIPS and SHINE using 110-μm Sachtopore sorbent.

Solution	Inner diameter (cm)	Length (cm)	Column volume (L)
Uranyl nitrate	12	9.7	1.1
Uranyl sulfate	12	13	1.5

the plant-scale column designs for both processes, which assume a uranium concentration between 100 and 150 g-U/L, a feed solution volume of 200–250 L, a Mo concentration near 10^{-5} M, and a 2-hour loading time. The plant-scale column design for SHINE is about 25% larger than for MIPS, which means slightly larger waste volumes.

3.4. Column Experiments and Mo Redox Chemistry. Mo oxidation state is a critical aspect of the separation and recovery process. Separation and recovery of Mo from a uranyl nitrate or uranyl sulfate solution assume that Mo is present as Mo(VI). However, the radiation environment surrounding these solutions is highly reducing and may alter Mo's oxidation state [1, 20, 27]. The likelihood for a change in Mo redox chemistry is much greater in a uranyl sulfate solution because nitrate is an oxidant, and if Mo were reduced, nitrate has the capacity to reoxidize it to Mo(VI). If Mo(VI) was reduced to Mo(V), it can be present as a cationic species, $Mo_2O_4^{2+}$, which will not adsorb on the Mo-recovery column [1, 9, 20, 27, 33, 34]. Because both MIPS and SHINE will be recycling their fuel/target solutions, adding an oxidant is not trivial. The redox potential for Mo(VI)/Mo(V) at pH = 0 is 0.50 V [33], but to what extent, in which system(s), and under what conditions will Mo reduction take place remains uncertain. Column experiments were initiated using the Van de Graaff as a source of constant radiation for uranyl sulfate solutions. Future experiments will use a linac as a constant source of radiation, and fission products will be generated.

Uranyl sulfate solutions were irradiated at the Van de Graaff under a constant radiation dose and passed through a titania column. Previous batch-study results where uranyl nitrate and uranyl sulfate solutions were irradiated at the Van de Graaff showed inconclusive results using sulfate solutions, but there was no observed reduction in Mo adsorption or recovery from nitrate solutions [20]. This is most likely due to the oxidizing behavior of nitrate. As a result, column experiments performed under a constant radiation dose were only performed using uranyl sulfate solutions. The focus of the constant-irradiation-column experiments shifted toward a sulfate media because it is a nonoxidizing environment in the absence of a radiation field. Mo oxidation state is more likely to change in a sulfate system than in a nitrate system. However, at solution dose rates of roughly 700 Gy/h, no changes in Mo redox chemistry were observed. Mo recoveries still ranged from 90 to 100%, and less than 1% Mo was found in the effluent stream, which suggests that Mo(VI) did not reduce to Mo(IV) or Mo(V) when exposed to dose rates in the 700 Gy/h range [21]. Table 3 shows the results from the column experiments performed under constant dose at the Van de Graaff. Errors associated with the gamma counting results for Mo-99 are ±7%, which explains why the total amount of Mo in all solutions does not sum 100%. In experiments where 1 M H_2SO_4 was used to wash the column, 11–15% Mo prematurely eluted during the acid and water washes because at lower pH values, Mo speciation changes from primarily a monoprotonated species, $HMoO_4^-$ [35], at pH 1 to a cationic species that does not adsorb as well on a titania sorbent.

Additional isotopes of concern for both processes were added to the target solutions prior to irradiation to gain a better understanding of their redox chemistry and speciation, which may help deduce where certain isotopes will end up postirradiation and post-Mo-99 recovery. Isotopes that were added to the target solution preirradiation included I-131 and Pu-239. Previous experiments with irradiated solutions showed that iodine contaminates the Mo-99 product prior to entry into the purification process. Iodine contamination in the Mo-99 product partially comes from decay of several Te isotopes, Te adsorbs, and Mo on a titania sorbent [9]. The distribution of isotopes during the separation and recovery processes is important for waste classification purposes. A clearer understanding of which fission products will be recycled to the target solution and which fission products will enter the purification process is needed. Modifications were made to the LEU Modified Cintichem purification process to account for the large amount of iodine, which has been found to coelute with the Mo-99 product [5, 13, 36]. An additional evaporation step using nitric acid was added to promote volatilization and capture of the iodine.

The current steps in the Cintichem process are capable of removing iodine and iodide but not iodate. Iodine speciation experiments at the Van de Graaff performed with uranyl nitrate and uranyl sulfate solutions suggested that all iodine species independent of starting species (iodine, iodide, and iodate were all tested, and isotopic equilibration was initiated with an I-131 spike) were reduced to iodide when exposed to low LET (linear energy transfer) particles [21]. These results are somewhat misleading because it is well known that iodine volatilizes in acidic solution and will most likely appear in multiple places during Mo-99 production, separation, recovery, and purification processes.

Column experiments were performed using a Pu-239 spike (added as Pu(IV)) to understand its behavior in the Mo-recovery process. More than half of the Pu-239 remained adsorbed on the column during the Mo-separation and recovery processes from an irradiated uranyl sulfate solution. Previous batch studies using a uranyl nitrate solution showed that Pu does adsorb on a titania sorbent [15]. Several options are viable for Pu removal from titania, but what, if any options are pursued to remove the Pu, will be dependent on the producer's needs. Results from column experiments performed using uranyl sulfate solutions and batch-contact studies performed using uranyl nitrate solutions suggest that a significant amount of Pu will remain adsorbed on the titania sorbent during the Mo separation and recovery process.

3.5. Gas Analysis Results and pH Changes from Van de Graaff Experiments. Initially, sodium nitrate and sodium sulfate solutions were irradiated using the Van de Graaff as

Table 3: Results for Van de Graaff column experiments.

Solution dose rate (Gy/h)	Column dose rate (Gy/h)	% Mo in effluent	% Mo in washes	% Mo in strip	Acid wash (M)
640	160	0.9	0.3	100	0.5
740	180	0.7	15	92	1
680	160	0.6	11	100	1
690	170	0.2	2	95	0.5

a radiation source [18]. Gases produced during irradiation were analyzed, and final pH measurements were taken postirradiation. After sodium salt irradiations were completed, a set of uranyl nitrate and uranyl sulfate solutions were irradiated at the Van de Graaff to measure gases produced and changes in pH. Postirradiated uranium solutions were also examined closely for possible precipitates. Production levels for hydrogen and oxygen gases as a function of radiation dose have been plotted. pH changes are much more significant in nitrate media and can lead to precipitation of fission products and uranium in the absence of a continuous feed of nitric acid. In sulfate media, pH changes are not that significant, but peroxide formation leads to the precipitation of uranyl peroxide if a catalyst to destroy peroxide is not added to the solution prior to irradiation [19].

3.6. Uranyl Nitrate Solutions. Irradiation of sodium nitrate and uranyl nitrate solutions at the Van de Graaff caused significant increases in pH postirradiation. As the nitrate concentration increased, the pH increased more significantly. The pH of a uranyl nitrate solution containing ~80 g-U/L did not change considerably postirradiation; however, as the concentration increased to 128 g-U/L, a final pH reading of 1.84 was measured (initial pH of 1.0). From previous experiments with irradiated uranyl nitrate solutions, fission products began to precipitate at a pH near 1.7 [35]. As the nitrate concentration increased even more (0.74 M and 0.95 M), the pH increased to ~2.2, which becomes a concern for uranium precipitation which occurs around a pH of 3.0 [1]. In similar irradiations with sodium nitrate solutions, the pH reached as high as 10.1 after a dose of $2.3E + 08$ Gy was applied to a solution containing 2.52 M NO_3^- [18].

The total production of hydrogen and oxygen was fairly consistent for uranyl nitrate solutions containing 128–226 g-U/L. A H_2/O_2 ratio between 1.2 and 1.4 was observed for the samples containing higher concentrations of uranyl nitrate, which correlates well with the increases in pH. For the solution containing roughly 80 g-U/L, the H_2 to O_2 ratio is much closer to 2 with a value of 1.75, which agrees with the fact that the pH did not change. Sodium nitrate solutions were also irradiated at the Van de Graaff (data not shown), and results were consistent with what was observed for uranyl nitrate solution irradiations. As the nitrate concentration increases for both sodium and uranyl nitrate solutions, the H_2/O_2 ratio decreases. This is most likely due to ammonia formation, which increases as nitrate increases and can reduce the amount of H_2 produced. These data for uranyl nitrate solutions are shown in Table 4 and Figures 2, 3, and 4.

Table 5 shows the detection of N_2O and NO during the irradiation of uranyl nitrate solutions at the Van de Graaff. In

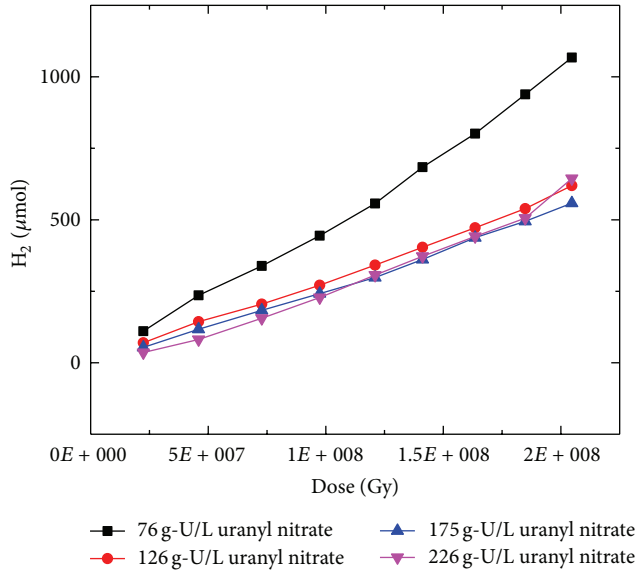

Figure 2: Hydrogen evolution measured during irradiation of $UO_2(NO_3)_2$ solutions at the Van de Graaff.

Table 5, ND indicates that the analyte was not detected during the experiment. The table shows the number of μmoles detected at each sampling time (t). These data are displayed in this fashion because the concentration of each analyte was below the lowest calibration standard utilized, even though peaks were still detected, and the NO_x compounds are very reactive. NO reacts with oxygen to form NO_2, which is a brown toxic gas. It also can react in the presence of oxygen and water to form nitrous acid, HNO_2. Considering the reactive nature of the NO_x species, it was decided that the best way to report the data are as total μmoles detected at time (t) instead of total accumulated μmoles. N_2O is only detected as a true peak (based on calibration standard) in the samples containing larger amounts of nitrate (175 g-U/L and 226 g-U/L).

3.7. Uranyl Sulfate Solutions. Table 6 shows the experimental data for the irradiation of uranyl sulfate solutions using the Van de Graaff accelerator as a source of radiation. Figures 5 and 6 show the total μmoles of each analyte (either hydrogen or oxygen) versus accumulated dose (Gy) during each five-hour experiment. The H_2/O_2 ratios are presented in Figure 7.

Uranyl peroxide precipitated during irradiation of uranyl sulfate solutions at the Van de Graaff accelerator. Density measurements were performed on the post-irradiated solutions after the precipitate was filtered to determine the

Table 4: Experimental data obtained from the irradiation of uranyl nitrate solutions at the Van de Graaff.

Uranium concentration (g-U/L)	Energy deposited (Gy)	Initial pH	Final pH	Total μmoles H_2 produced	Total μmoles O_2 produced	G value H_2 (H_2/100 eV)	G value O_2 (O_2/100 eV)	H_2 to O_2 ratio
76	2.32E + 08	1.0	1.02	1240	710	0.025	0.015	1.75
128	2.33E + 08	1.0	1.84	690	490	0.014	0.010	1.41
175	2.32E + 08	1.0	2.21	650	520	0.013	0.011	1.24
226	2.05E + 08	1.0	2.09	650	550	0.015	0.013	1.17

Table 5: N_2O and NO in μmoles measured at sampling time for irradiated uranyl nitrate solutions.

Sampling time (min)	76 g-U/L		128 g-U/L		175 g-U/L		226 g-U/L	
	N_2O	NO	N_2O	NO	N_2O	NO	N_2O	NO
30	<0.5	<0.5	<0.5	<0.5	<0.5	<0.5	<0.5	<0.5
60	<0.5	<0.5	<0.5	<0.5	<0.5	<0.5	<0.5	<0.5
90	<0.5	<0.5	<0.5	<0.5	<0.5	<0.5	<0.5	<0.5
120	<0.5	<0.5	<0.5	<0.5	<0.5	<0.5	1.52	<0.5
150	<0.5	<0.5	<0.5	<0.5	<0.5	<0.5	3.05	<0.5
180	<0.5	<0.5	<0.5	<0.5	<0.5	<0.5	3.96	<0.5
210	<0.5	<0.5	<0.5	<0.5	1.32	<0.5	4.17	<0.5
240	<0.5	<0.5	<0.5	<0.5	2.84	<0.5	2.64	<0.5
270	<0.5	<0.5	<0.5	<0.5	2.24	<0.5	3.35	<0.5
300	<0.5	<0.5	<0.5	<0.5	2.03	<0.5	N.D.	N.D.

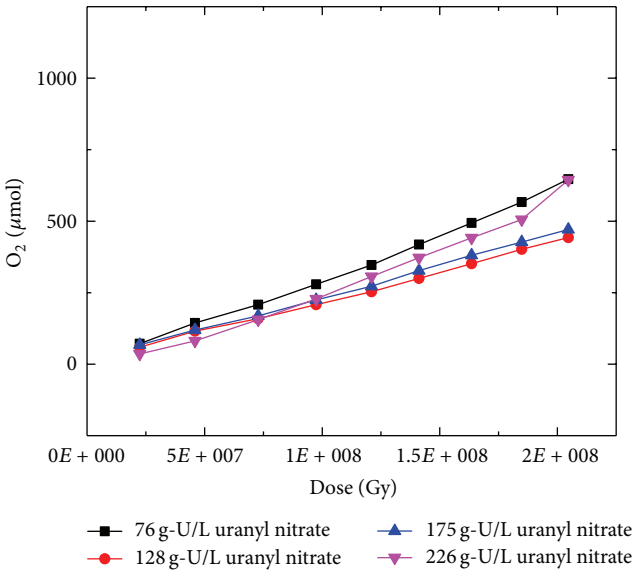

Figure 3: Oxygen evolution measured during irradiation of $UO_2(NO_3)_2$ solutions at the Van de Graaff.

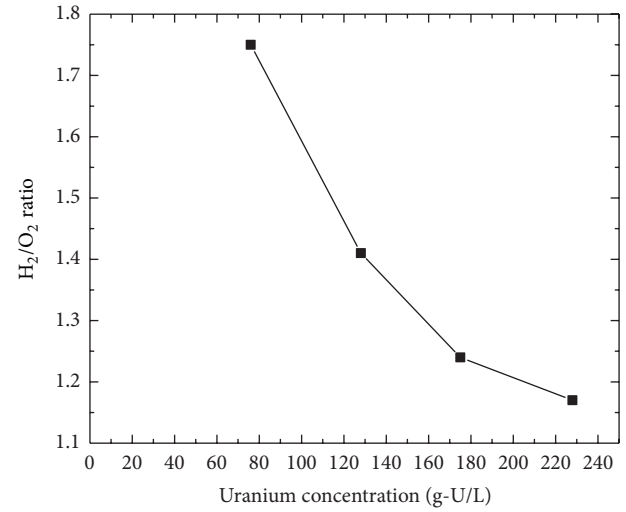

Figure 4: Hydrogen to oxygen ratios measured for uranyl nitrate solutions during irradiation tests at the Van de Graaff.

approximate amount of uranium that had precipitated. Uranium concentrations decreased by ~22–36 g-U/L for postirradiated uranyl sulfate solutions. Those data are shown in Table 6. Precipitated uranium can be redissolved by destruction of peroxide at elevated temperatures.

The pH values for the postirradiated uranyl sulfate solutions decreased, which is due to the formation of uranyl peroxide and loss of H_2O from radiolysis. Sodium sulfate solutions were also irradiated at the Van de Graaff, but no precipitates were observed because sodium peroxide is soluble; however, the pH values of the postirradiated sodium sulfate solutions decreased as well.

The production of hydrogen and oxygen was high for all of the uranyl sulfate irradiation experiments. These data are consistent with results obtained from irradiation of sodium sulfate solutions at the Van de Graaff (data not shown), where H_2/O_2 ratios increased as the concentration of sulfate increased. The ratio of $H_2 : O_2$ was at or slightly above 2 : 1,

Table 6: Experimental data obtained from the irradiation of uranyl sulfate solutions at the Van de Graaff.

Initial uranium conc. (g-U/L)	Energy deposited (Gy)	Final uranium conc. (g-U/L)	Initial pH	Final pH	Total μmoles H_2 produced	Total μmoles O_2 produced	G value H_2 (H_2/100 eV)	G value O_2 (O_2/100 eV)	H_2 to O_2 ratio
88	1.71E + 08	63.5	1	0.64	2972	1446	0.082	0.0399	2.05
138	2.29E + 08	116	1	0.63	1320	634	0.0278	0.0134	2.08
298	2.03E + 08	262	1	0.58	1092	459	0.0259	0.0109	2.38

Table 7: Experimental data obtained from the irradiation of uranyl sulfate solutions in the presence of potential peroxide catalysts at the Van de Graaff.

Catalyst	Uranium concentration (g-U/L)	Energy deposited (Gy)	Did sample precipitate	Total μmoles H_2 produced	Total μmoles O_2 produced	H_2 to O_2 ratio
Cu(II), 62.5 mg-Cu/L	126	2.20E + 08	No	410	290	1.42
KI, 9.94 mg-I/L	126	2.28E + 08	No	210	150	1.40
Fe(III), 0.96 mg-Fe/L	126	2.28E + 08	No	570	370	1.53
304 stainless steel	126	2.24E + 08	No	260	220	1.17
Zirconium	298	2.32E + 08	Yes	1110	460	2.42

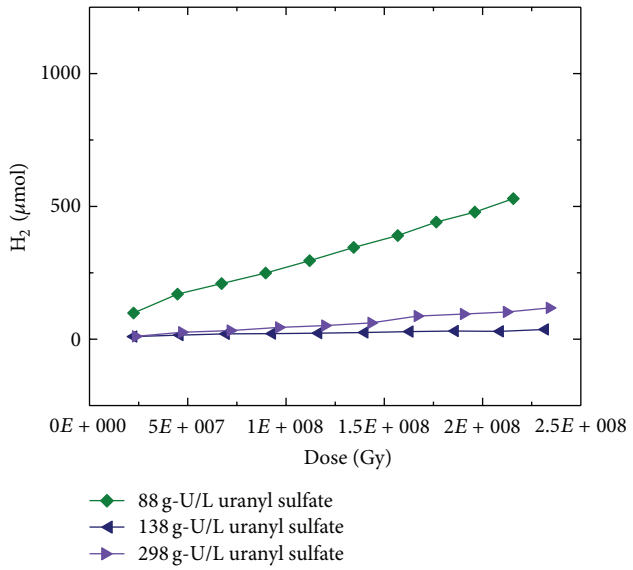

Figure 5: Hydrogen evolution measured during irradiation of UO_2SO_4 solutions at the Van de Graaff.

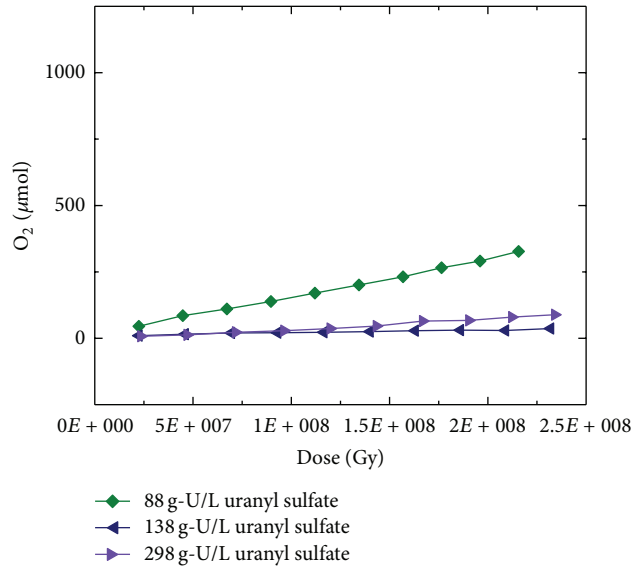

Figure 6: Oxygen evolution measured during irradiation of UO_2SO_4 solutions at the Van de Graaff.

favoring production of hydrogen as sulfate increased in sodium and uranyl sulfate solutions. Despite the fact that the H_2/O_2 ratio is close to 2.0 (theoretical value for water) for the 88 g-U/L uranyl sulfate sample, peroxide was still being formed because the pH decreased and a precipitate formed.

3.8. Catalytic Destruction of Peroxide in Uranyl Sulfate Solutions. To prevent precipitation of uranyl peroxide, a catalyst must be added to the uranyl sulfate solution prior to irradiation to decrease the steady-state concentration of radiolytically generated hydrogen peroxide. Fe(II) added as $FeSO_4$ has been shown to accomplish this at concentrations as low as 1 ppm. In order to expand the available options for use in the SHINE system, other salts were tested because of their known ability to catalyze destruction of H_2O_2. Experiments were performed using aqueous solutions of copper(II) sulfate, potassium iodide, and iron(III) sulfate [37]. Potential target solution vessel materials, 304 stainless steel and zirconium ASME 658, were also tested. The stainless steel and Zr were added as solid turnings to 2 mL of ~130 g-U/L uranyl sulfate solution.

Table 7 and Figures 8–10 show experimental data for the irradiation of uranyl sulfate solutions containing the potential H_2O_2 destruction catalysts discussed above. Each sample contained a different catalyst at the concentration shown. Figures 8 and 9 show the total μmoles of each analyte

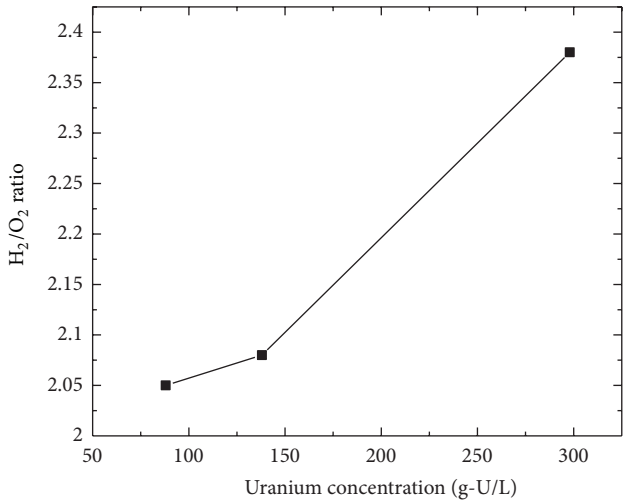

FIGURE 7: Hydrogen to oxygen ratios measured for UO_2SO_4 solutions during irradiation tests at the Van de Graaff.

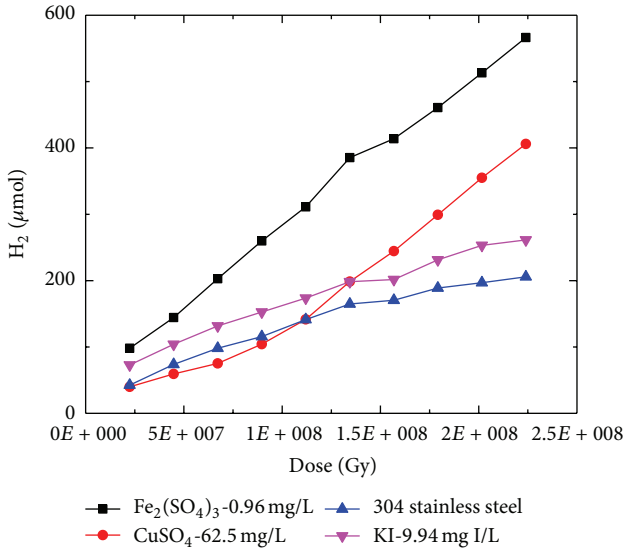

FIGURE 8: Hydrogen evolution measured during irradiation of 126 g-U/L UO_2SO_4 solutions in the presence of potential peroxide catalysts at the Van de Graaff.

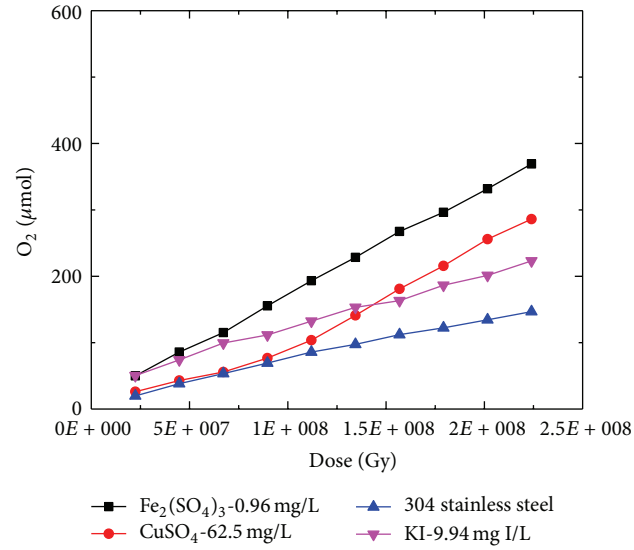

FIGURE 9: Oxygen evolution measured during irradiation of 126 g-U/L UO_2SO_4 solutions in the presence of potential peroxide catalysts at the Van de Graaff.

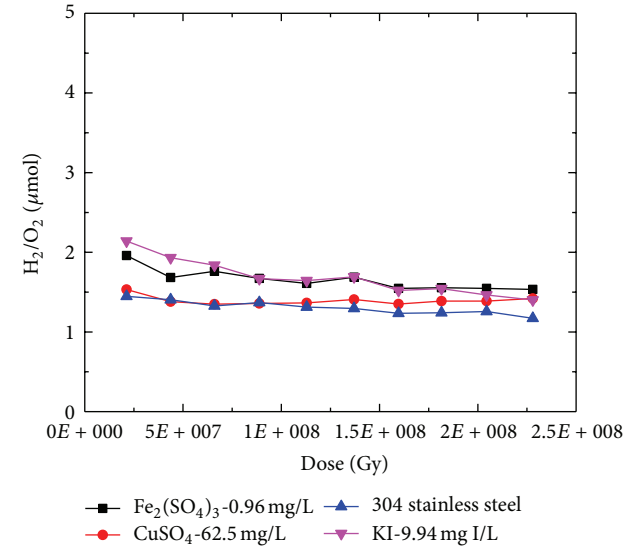

FIGURE 10: Hydrogen to oxygen ratios measured during irradiation of 126 g-U/L UO_2SO_4 solutions in the presence of potential peroxide catalysts at the Van de Graaff.

(either hydrogen or oxygen) versus accumulated dose (Gy) at sampling time during each five-hour experiment. Figure 10 presents the H_2-to-O_2 ratios versus dose for the data. Comparing Tables 6 and 7, it is evident that the addition of a peroxide catalyst reduces the overall gas production and changes the H_2-to-O_2 ratio from ~2 : 1 to ~1.4 : 1.

Zr metal was not effective at preventing precipitation of uranyl peroxide, so if the target solution vessel for SHINE is made of Zr, an additional catalyst would most likely be required to accelerate peroxide destruction. Irradiated uranyl sulfate solutions containing Zr metal exhibited similar behavior to the irradiated uranyl sulfate solutions where uranyl peroxide precipitated. High volumes of hydrogen and oxygen were generated, and H_2-to-O_2 ratios greater than 2 were observed.

The solution containing 304 stainless steel turnings showed no evidence of precipitation, but the exact mechanism of destruction is unknown. It may be a surface effect or through dissolution of reactive ions. The 304 stainless steel test showed low overall gas production and a low $H_2 : O_2$ ratio. The $H_2 : O_2$ ratio was 1.17, which is the lowest ratio observed for any of the uranyl sulfate solutions irradiated with effective catalysts, but the ratio is similar to uranyl nitrate solutions containing higher concentrations of U (175 g-U/L

and 226 g-U/L, see Table 4) that were irradiated at the Van de Graaff.

Irradiations with the metal salt catalysts (copper sulfate, potassium iodide, and ferric sulfate) were also effective at preventing precipitation of uranyl peroxide. All of the salt catalysts reduced the overall gas production and reduced the H_2-to-O_2 ratios to values below 2, but the ratios were still larger than the ratio of 1.17 observed for the uranyl sulfate solution containing the 304 stainless steel turnings.

4. Conclusions

Uranyl nitrate solutions are easier to prepare than uranyl sulfate solutions, but large pH increases are observed upon irradiation. A continuous feed of nitric acid is required to prevent precipitation of uranium and fission products during irradiation. Uranyl sulfate solutions are more difficult to prepare, but large pH increases are not observed upon irradiation. However, a catalyst is required to promote peroxide destruction and prevent precipitation of uranyl peroxide.

Mo recovery is a slightly easier from nitrate media compared to sulfate media. This is due to the fact that sulfate competes more strongly with molybdenum for titania adsorption sites than nitrate. A plant-scale Mo recovery column would be about 25% larger for a uranyl sulfate solution compared to a uranyl nitrate solution. From a neutronics standpoint, uranyl sulfate is preferred due to the fact that nitrogen absorbs thermal neutrons, which creates a loss of neutrons, and decreases the overall reactivity. There are advantages and disadvantages associated with both uranyl salts, but Mo-99 separation and recovery using a titania sorbent followed by Mo-99 purification using the LEU-Modified Cintichem process are feasible using a uranyl sulfate or uranyl nitrate target solution.

Acknowledgment

This work is supported by the US Department of Energy, National Nuclear Security Administration's (NNSA's) Office of Defense Nuclear Nonproliferation, under Contract DE-AC02-06CH11357.

References

[1] IAEA(International Atomic Energy Association)-TECDOC-1601, *Homogeneous Aqueous Solution Nuclear Reactors for the Production of Mo-99 and Other Short Lived Radioisotopes*, Vienna, Austria, 2008.

[2] G. Piefer, "Mo-99 production using a subcritical assembly," in *Proceedings of the 1st Annual Mo-99 Topical Meeting*, Santa Fe, NM, USA, December 2011.

[3] K. M. Pitas, G. R. Piefer, R. V. Bynum, E. N. Van Abel, and J. Driscoll, "SHINE: technology and progress," in *Proceedings of the Mo-99 Topical Meeting on Molybdenum-99 Technological Development*, Chicago, Ill, USA, April 2013.

[4] A. J. Bakel, S. B. Aase, A. A. Leyva, K. J. Quigley, and G. F. Vandegrift, "Thermoxid sorbents for the separation and purification of ^{99}Mo," in *Proceedings of the International RERTR Meeting*, Vienna, Austria, November 2004.

[5] A. J. Bakel, D. C. Stepinski, G. F. Vandegrift et al., "Progress in technology development for conversion of ^{99}Mo production-BATAN'S (INDONESIA) conversion program, progress in the CNEA (Argentina) LEU foil/baseside process, and development of inorganic sorbents for ^{99}Mo production," in *Proceedings of the International RERTR Meeting*, Boston, Massa, USA, November 2005.

[6] G. F. Vandegrift, A. J. Bakel, and J. W. Thomas, "Overview of 2007 ANL progress for conversion of HEU-based Mo-99 production as part of the U.S. Global Threat Reduction—Conversion Program," in *Proceedings of the International RERTR Meeting*, Prague, Czech Republic, September 2007.

[7] G. F. Vandegrift, J. Fortner, A. J. Bakel et al., "Overview of argonne progress related to implementation of Mo-99 production by use of a homogeneous reactor," in *Proceedings of the International RERTR Meeting*, Washington, DC, USA, October 2008.

[8] A. J. Ziegler, D. C. Stepinski, J. F. Krebs, S. D. Chemerisov, A. J. Bakel, and G. F. Vandegrift, "Mo-99 recovery from aqueous-homogeneous-reactor fuel—behavior of termoxid sorbents," in *Proceedings of the International RERTR Meeting*, Washington, DC, USA, October 2008.

[9] D. Stepinski, A. Ziegler, J. Jerden et al., "Sorbent selection progress report," ANL/CSE-13/16, Argonne National Laboratory, 2009.

[10] G. F. Vandegrift, D. C. Stepinski, A. J. Ziegler et al., "Overview of argonne progress in developing LEU-based processes for the production of Mo-99," in *Proceedings of the International RERTR Conference*, Beijing, China, November 2009.

[11] E. O. Krahn, A. S. Hebden, G. F. Vandegrift, P.-L. Chung, and L. Wang, "Mechanical stability study," ANL/CSE-13/3, Argonne National Laboratory, 2010.

[12] A. J. Youker, P.-L. Chung, E. O. Krahn, D. C. Stepinski, A. V. Gelis, and G. F. Vandegrift, "Mo-99 stripping results and column designs for Mini-Medical Isotope Production System (MIPS)," ANL/CSE-13/15, Argonne National Laboratory, 2011.

[13] A. J. Youker, P.-L. Chung, P. Tkac et al., "Separation, purification, and clean-up developments for MIPS and SHINE," in *Proceedings of the 1st Annual Mo-99 Topical Meeting*, Santa Fe, NM, USA, December 2011.

[14] A. J. Youker, P.-L. Chung, E. O. Krahn, and G. F. Vandegrift, "Column optimization studies," ANL/CSE-13/2, Argonne National Laboratory, 2012.

[15] A. J. Youker, D. C. Stepinski, L. Ling, and G. F. Vandegrift, "Mo recovery updates and physical properties of Uranyl sulfate solutions," ANL/CSE-13/20, Argonne National Laboratory, 2012.

[16] A. J. Youker, D. C. Stepinski, M. Kalensky et al., "Progress Related to Mo-99 Separation, Precipitation Prevention, and Clean-Up for SHINE System," in *Proceedings of the Topical Meeting on Molybdenum-99 Technological Development*, Chicago, Ill, USA, April 2013.

[17] C. Milhano and D. Pletcher, "The electrochemistry and electrochemical technology of Nitrate," *Modern Aspects of Electrochemistry*, vol. 45, pp. 1–61, 2009.

[18] M. Kalensky, S. Chemerisov, A. Youker et al., "Radiolysis of nitrate and sulfate solutions," ANL/CSE-13/23, Argonne National Laboratory, 2012.

[19] M. Kalensky, S. Chemerisov, A. Youker et al., "Means to eliminate uranyl peroxide in SHINE target solution," ANL/CSE-13/21, Argonne National Laboratory, 2013.

[20] A. Gelis, S. Chemerisov, A. Bakel, and G. Vandegrift, "Radiolysis effects on molybdenum oxidation state and recovery

from aqueous-homogeneous-reactor fuel," in *Proceedings of the International RERTR Meeting*, Washington, DC, USA, October 2008.

[21] A. Youker, J. Krebs, A. Hebden, K. Quigley, D. Stepinski, and G. Vandegrift, "Van de graaff experiments: Mo redox chemistry and iodine speciation," ANL/CSE-13/17, Argonne National Laboratory, 2012.

[22] I. Draganic', "Oxalic Acid: the only aqueous dosimeter for In-Pile use," *Nucleonics*, vol. 21, pp. 33–35, 1963.

[23] C. A. Laue, D. Gates-Anderson, and T. E. Fitch, "Dissolution of metallic uranium and its alloys. Part I. Review of analytical and process-scale metallic uranium dissolution," *Journal of Radioanalytical and Nuclear Chemistry*, vol. 261, no. 3, pp. 709–717, 2004.

[24] J. A. Lane, "Properties of aqueous fuel solutions," in *Aqueous Homogeneous Reactors*, chapter 3, pp. 85–123, Oak Ridge National Laboratory, 1958.

[25] G. F. Vandegrift, "Transformation of urex effluents to solid oxides by concentration, denitration, and calcination," Tech. Rep. ANL-00/25, Argonne National Laboratory, 2000.

[26] A. J. Bakel and G. F. Vandegrift, "Equipment and method choices for concentration and denitration of the uranium product from UREX," ANL/CSE-13/1, Argonne National Laboratory, 2013.

[27] G. E. Dale, D. A. Dalmas, M. J. Gallegos et al., "^{99}Mo separation from high-concentration irradiated Uranium Nitrate and Uranium sulfate solutions," *Industrial and Engineering Chemistry Research*, vol. 51, pp. 13319–13322, 2012.

[28] H. L. Anderson, "High power water boiler," LA-394, Los Alamos National Laboratory, 1945.

[29] H. M. Busey, "Composition and decontamination of residual water-boiler off-gas," LA-1521, Los Alamos National Laboratory, 1953.

[30] P. R. Kasten, *Reactor Dynamics of the Los Alamos Water Boiler*, vol. 50 of *C.E.P. Symposium*, Nuclear Engineering, 1954.

[31] S. Klein, "Effects of solution chemistry on aqueous reactor (AHR) reactivity," LA-UR 10-04317, Los Alamos National Laboratory, 2010.

[32] J. A. Berninger, R. D. Whitley, X. Zhang, and N.-H. L. Wang, "A versatile model for simulation of reaction and nonequilibrium dynamics in multicomponent fixed-bed adsorption processes," *Computers and Chemical Engineering*, vol. 15, no. 11, pp. 749–768, 1991.

[33] Olleman-Wiberg, *Inorganic Chemistry*, Academic Press, 1995.

[34] Spinks and Woods, *Introduction to Radiation Chemistry*, John Wiley & Sons, 1990.

[35] J. Jerden, J. Kropf, A. Bakel, and G. Vandegrift, "Speciation and concentration of metals in a homogeneous reactor fuel solution," ANL/CSE-13/7, Argonne National Laboratory, 2009.

[36] A. Bakel, A. Leyva, T. Wiencek et al., "Overview of progress related to implementation of the LEU-Modified cintichem process," in *Proceedings of the International RERTR Meeting*, Washington, DC, USA, October 2008.

[37] J. H. Baxendale, "Decomposition of hydrogen peroxide by catalysts in homogeneous aqueous solution," *Advances in Catalysis*, vol. 4, no. C, pp. 31–86, 1952.